Respiratory Physiology & Neurobiology 216 (2015) 1–8

Contents lists available at ScienceDirect

Respiratory Physiology & Neurobiology

journal homepage: www.elsevier.com/locate/resphysiol

Bubble size on detachment from the luminal aspect of ovine large blood vessels after decompression: The effect of mechanical disturbance

Ran Arieli [a,*], Uri Arieli [b], Abraham Marmur [c]

[a] Israel Naval Medical Institute, Israel Defence Forces Medical Corps, Haifa, Israel
[b] Department of Physics, Tel Aviv University, Tel Aviv, Israel
[c] Department of Chemical Engineering, Technion-Israel Institute of Technology, Haifa, Israel

ARTICLE INFO

Article history:
Received 31 March 2015
Received in revised form 29 April 2015
Accepted 1 May 2015
Available online 21 May 2015

Keywords:
Decompression bubble
Hydrophobic spot
Arterial bubbles
Pulsatile flow

ABSTRACT

Bubbles nucleate and develop after decompression at active spots on the luminal aspect of ovine large blood vessels. Series of bubbles were shown to detach from the active spot with a mean diameter of 0.7–1.0 mm in calm conditions. The effect of mechanical disturbance (striking the bowl containing the vessel or tangential flow) was studied on ovine blood vessels stretched on microscope slides and photographed after hyperbaric exposure. Diameter on detachment after a heavy blow to the bowl was 0.87 ± 0.43 mm (mean $\pm$ SD), no different from bubbles which detached without striking the bowl (0.86 ± 0.28 mm). Bubble diameter on detachment during pulsatile tangential flow at 234 cm/min, 0.99 ± 0.36 mm, was not smaller than that seen in the same blood vessels in calm conditions (0.81 ± 0.34 mm). The active spots were stained for lipids, proving their hydrophobicity. The most abundant active spots, which produced only a few bubbles, did not stain for lipids thereafter. The possibility that phospholipids were removed along with detached bubbles may correlate with acclimation to diving. The finding of bubble production at the active spots matches observed phenomena in divers: variable sensitivity to decompression, acclimation to diving, the effect of elevated gas load on increased bubble formation, a higher bubble score in the second dive on the same day, and unexplained neurological symptoms after decompression. Large bubbles released from the arterial circulation give serious cause for concern.

1. Introduction

It has been shown that tiny, flat gas nanobubbles measuring 5–100 nm form spontaneously when a smooth hydrophobic surface is submerged in water containing dissolved gas (Tyrrell and Attard, 2001; Yang et al., 2007). In our previous studies (Arieli and Marmur, 2011, 2013a), these nanobubbles were shown to be the source of gas micronuclei from which bubbles evolved during decompression on smooth hydrophobic silicon wafers.

We have also shown that hydrophobicity on the luminal aspect of ovine large blood vessels, the aorta (AO), pulmonary artery and vein (PA, PV), superior vena cava (VC) and right and left atrium, may be the source of bubble nucleation and growth following decompression of a stretched blood vessel under saline (Arieli and Marmur, 2013b).

We further found (Arieli and Marmur, 2014) that there are active spots on the luminal aspect of ovine large blood vessels (AO, PA, PV and VC) at which bubbles nucleate and develop after decompression. Each spot produced a series of bubbles after decompression, and the occurrence of these spots was highly variable within the vessels and between sheep. Under calm conditions, bubbles detached from the active spot with a mean diameter of 0.7–1.0 mm. The calculated attachment force between the bubble and the active spot was 4.5×10^{-5} N. Bubbles as large as this in the arterial circulation (AO, PV and left atrium), could have a serious effect on the central nervous system.

However, conditions in vivo are not calm at all; pulsed blood flow may sweep bubbles off the luminal aspect of the vessel before they develop and grow. Using hydrophobic silicon wafers, we showed that the tangential force for detachment of a bubble was half the normal force (Arieli and Marmur, 2013b). If this were true for a blood vessel, the bubble would become detached when the tangential force applied by the flow exceeded half the normal force for detachment.

* Corresponding author. Tel.: +972 77 8100825; fax: +972 4 9801210.
E-mail address: rarieli@netvision.net.il (R. Arieli).

http://dx.doi.org/10.1016/j.resp.2015.05.001
1569-9048/

The purpose of the present study was to investigate the actual attachment force and bubble size on detachment when a mechanical disturbance was produced. The pulse effect of in-vivo blood flow was imitated by administering a heavy blow to the Pyrex bowel containing the vessel. The effect of flow was studied by recirculating the supersaturated saline to produce horizontal, pulsatile flow over the stretched blood vessel. We have previously demonstrated both local hydrophobicity (Arieli and Marmur, 2014) and bubble production from active spots in large blood vessels of the sheep (Arieli and Marmur, 2013b); however, hydrophobicity was not proved for the active spots. This was now done by staining the blood vessel for lipids after the location of active spots by observing their bubble production, and the search for a match between lipid staining and the active spots.

2. Methods

2.1. Tissue preparation

The complete heart and lungs from 12 slaughtered sheep (taken on separate days) were obtained at the abattoir, and on removal intact from the thoracic cavity were immediately immersed in a cooler filled with saline. In the laboratory, under saline and without any exposure to air, samples (area $10.1 \pm 2.2\ cm^2$, mean ± SD) from the PA, PV, AO and VC, were gently stretched on microscope slides using metal clips with the luminal aspect exposed. Because the metal clips tended to rust during the exposure they were stained with anti-rust. Two slides were placed without exposure to air on the bottom of two Pyrex bowls (diameter 26 cm, height 5 cm) under 2.5 cm saline. The other two slides were kept under saline in the refrigerator for the next day.

2.2. General protocol

2.2.1. Procedure

The bowls containing the samples were transferred to two different 150-l hyperbaric chambers (Roberto Galeazzi, La Spezia, Italy). Pressure was elevated at a rate of 200 kPa/min to 1013 kPa, 90 metres sea water (msw), and remained at that pressure overnight (20.5 ± 2.3 h, mean ± SD). This prolonged exposure and high pressure were needed because of the long diffusion distance, in order to achieve an appreciable gas concentration near the vessel. This was calculated using mirror and Gaussian functions (Appendix 1). For example, gas tension after 20 h was calculated to amount to 228 kPa (13 msw) near the blood vessel.

In the morning, one of the chambers was decompressed at a rate of 200 kPa/min. The bowl was placed carefully on a nearby table for photography. We immediately started automated photographing (Canon EOS 500d with a macro lens 100 mm, F/2.8 EF USM), at 1-s intervals for one hour. After the first 30 min of photography, the battery and memory card were replaced and photography was resumed for the second 30 min. The 1-h sampling time was chosen because we found previously that after an hour the rate of bubble production began to drop (Arieli and Marmur, 2013b). At the end of the 1 h of photography, the slides with the tissues were removed and photographed against graph paper for later scaling.

The same protocol was followed for the bowl in the second chamber, for the remaining two blood vessel samples from the same animal, and for the samples from each of the other sheep.

2.2.2. Staining

The slides with the blood vessels were preserved in formalin (10% formaldehyde). Vessels were later stained for lipids using Oil Red O (Sudan III, S4136-25G, Sigma Aldrich, St. Louis, MO, USA). Blood vessels were rinsed with distilled water and immersed in propylene glycol. The dye was prepared according to the instructions: dye in propylene glycol was stirred while being heated to 95 °C, filtered, and left overnight before the second filtering. After 20 min under the dye solution the vessels were immersed in 85% propylene glycol, after which they were rinsed in distilled water. Vessels were then photographed.

2.2.3. Diameter on detachment

The photographs of each sample were examined in sequence until detachment of a bubble was observed, and the time was noted. The camera was focused on the tissue-saline interface, and when a bubble detached and started floating upwards it went out of focus (for details see Arieli and Marmur, 2014). Bubbles produced near the edges of the tissue were not taken into consideration, and therefore the last 1 mm to the edge of the tissue was not included in the analysis. The area of the blood vessel samples and the diameter of a bubble just before detachment were measured using an image processing programme (Image-Pro-Plus, Media Cybernetics Inc., Bethesda, MD, USA).

2.3. Bowl-striking protocol

Samples from 6 sheep were used in this protocol. At 20, 40 and 55 min from the end of decompression, the bowl was struck a heavy vertical blow with a metal rod. Care was taken not to cause damage to the bowl. This blow caused bubbles outside the blood vessel to float upwards, and such a blow would certainly cause bubbles to rise in a carbonated drink. Before the blow was delivered, the metal rod was presented for 1 s to the camera to mark the timing. This was followed immediately by the blow being struck. The diameter of bubbles which detached within 2 s of the blow being delivered were compared with the diameter on detachment measured in calm conditions.

2.4. Tangential flow protocol

For the saline flow, we used a peristaltic pump producing a flow of 100–1000 ml/min (Major Science, MU-D01, Saratoga, CA, USA). The flow was pulsatile and therefore closely imitated pulsatile arterial flow. The actual flow was calibrated, and was linearly related to the number of revolutions per minute (rpm). A funnel-shaped bottle was placed next to the slide with the stretched blood vessel. Outflow from the bottle was via a horizontal slit 5 mm high and 5.5 cm wide, with the lower edge of the slit facing the vessel and close up to it. The saline was delivered in a horizontal flow over the blood vessel (lower panel, Fig. 1). A metal weight was placed above a hole in the top of the funnel-shaped bottle to prevent it floating, and once in a while was raised to allow the release of accumulated gas. When in place, the weight plugged the hole.

The range of systemic blood flow velocities in the dog was calculated from data presented by Snyder (1973), and is shown in the upper panel of Fig. 1. A preliminary test with saturated saline and a flow velocity of about 500 cm/min (300 rpm) produced a great number of bubbles, which would have masked the slide and probably have depleted the amount of dissolved gas in the saline. We therefore selected a flow of 234 cm/min (150 rpm), which produced much fewer bubbles. Most of these were trapped at the top of the funnel-shaped bottle, while the rest could be removed by careful use of a suction tube. The velocity we selected is greater than that present in most blood vessels, except for the large arteries and the VC (upper panel, Fig. 1).

The first 30 min of photography were conducted in calm conditions. Because there was an interval of a few minutes between the first and second photography sessions, photography in the second session started ahead of flow activation in order to obtain at least two shots of the vessel in calm conditions before flow

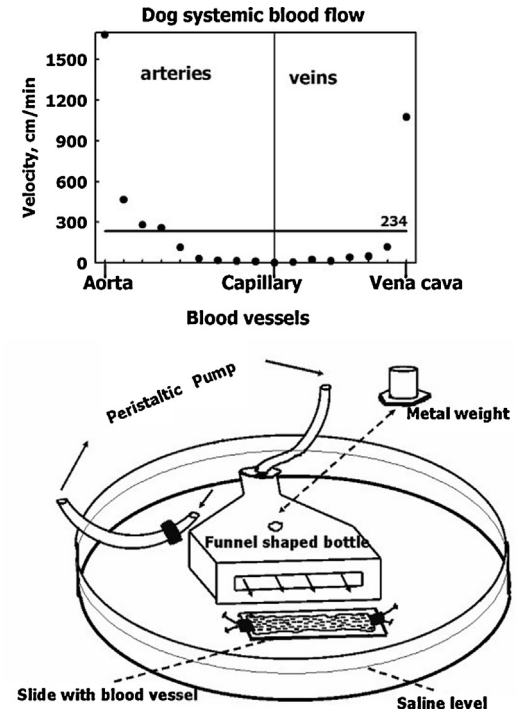

Fig. 1. The experimental system for studying the effect of tangential flow (lower panel), and blood flow velocities in the systemic circulation of the dog as calculated from Snyder (1973) (upper panel). The saline flow velocity we selected for the study is shown by the horizontal line.

activation. This protocol enabled us to compare diameter on detachment during the transition from the calm regime to flow conditions.

Activating the pump should have two opposing effects on the availability of dissolved gas in the vicinity of the blood vessel: (1) Enhancing the release of dissolved gas from the saline due to the bubbles formed at the pump. (2) Mixing of saline from the top, which was rich in gas, with saline from the bottom which was pure gas (Appendix 1), should result in elevation of the gas concentration close to the vessel wall.

2.5. Statistics

The Kolmogorov–Smirnov test was used for checking normality of the data. Two groups of bubbles on detachment, bubble production, and active-spot abundance were then compared using either the *t*-test or the Mann–Whitney test. The specific effects of individual sheep, blood vessels or active spots were tested using univariate analysis of variance.

3. Results

Bubble size on detachment is presented for the bowl-striking and tangential flow protocols. We then go on to describe the nature of the active spots and the findings from lipid staining in the two protocols. Finally, the variability in bubble production between sheep and blood vessels is presented on the basis of the two protocols employed in the present study and a previous report, a total of 19 animals.

3.1. Bubble detachment in the bowl-striking protocol

In two sheep bubbles were produced by only one of the four vessels, in three sheep by only two, and in one sheep by three of the four vessels. Bubbles were produced in the AO, PV, and VC in two sheep and in the PA in four sheep. Bubbles were produced at defined active spots (Arieli and Marmur, 2014).

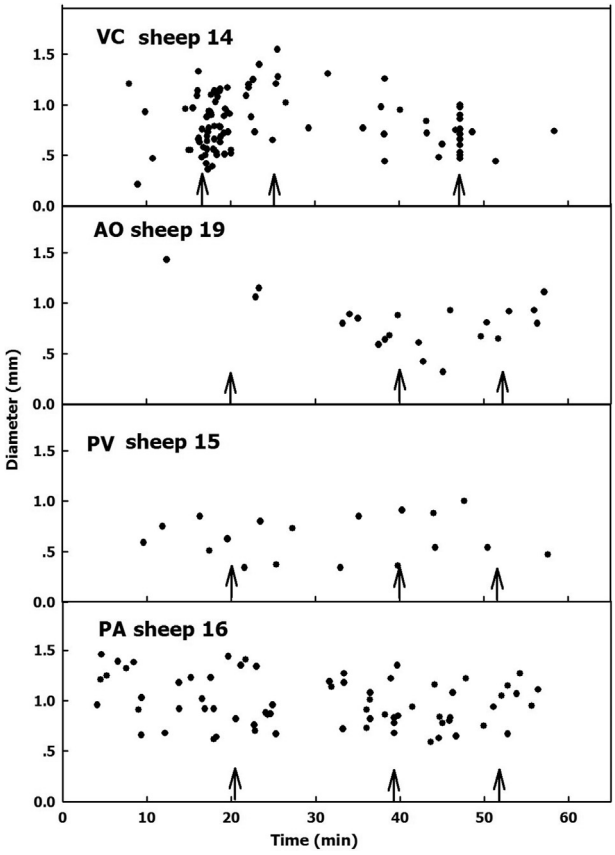

Fig. 2. Diameter of bubbles on detachment (bowl-striking protocol) plotted as a function of time from decompression for four blood vessels with high bubble production: VC, superior vena cava; AO, aorta; PV, pulmonary vein; PA, pulmonary artery. Sheep number and the blood vessel are noted for each panel. Arrows represent blows delivered to the bowl.

An example of the diameter of bubbles on detachment from blood vessels representative of the four sampled vessels, each with the highest bubble production for the vessel of its kind, is shown in Fig. 2. The striking was mistimed for the VC in sheep 14 (upper panel). Large numbers of bubble detachments were observed for the VC of sheep 14 after the bowl was struck, but this was the only clear case in 10 bubble-producing blood vessels. The large number of detachments within 3 min of the first blow in this vessel could be due to a mutual interaction between neighbouring bubbles. The bubbles which became detached from the VC in sheep 14 following the blow to the bowl were no smaller than the other detached bubbles. The diameter of all detached bubbles (mean ± SD) was 0.75 ± 0.25 mm ($n = 31$) for the AO, 0.94 ± 0.30 mm ($n = 145$) for the PA, 0.73 ± 0.25 mm ($n = 26$) for the PV and 0.81 ± 0.26 mm ($n = 120$) for the VC.

To test the direct effect of a blow delivered to the bowl on the diameter of the detached bubbles, their diameter during the 2 s following the blow was compared with all other diameters on spontaneous detachment. A comparison was also made with the diameter of stable bubbles, which were on the surface of the vessel 1 s before the blow and adhered to the spot, remaining in place for more than 2 s after the blow had been delivered. This comparison was intended to evaluate which of the available bubbles were affected by the blow delivered to the bowl. Results from all the bubble-producing vessels from 6 sheep ($n = 9$) are shown in Fig. 3, in which the percentage of bubbles is given as a function of 0.5 mm diameter bins. We omitted to photograph the metal rod for the VC

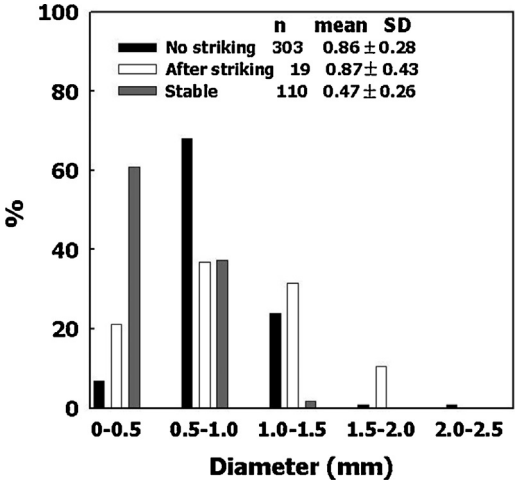

Fig. 3. Percentage distribution by diameter (0.5 mm bins) of bubbles which became detached following a blow delivered to the bowl: within 2 s of the blow (empty bars), spontaneously (black bars), and bubbles which were not affected by the blow to the bowl and remained stable (grey bars). Number of bubbles, mean diameter and SD are shown.

in sheep 14, which was therefore excluded from this analysis. The highest percentage of stable bubbles was in the 0–0.5 mm bin, and this decreased to moderate in the 0.5–1.0 mm bin, and to a small percentage in the 1.0–1.5 mm bin. The diameter of stable bubbles was different from the blow-related detached bubbles ($P < 0.001$). None was observed in bins above the third.

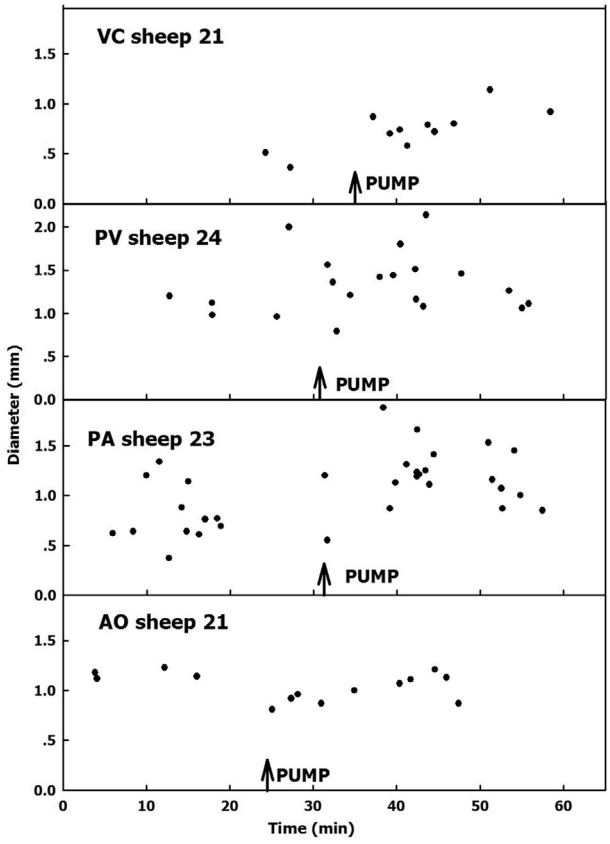

Fig. 4. Diameter of bubbles on detachment (tangential flow protocol) plotted as a function of time from decompression for four blood vessels which produced bubbles in both calm and flow conditions. Other symbols are as in Fig. 2. Arrows represent pump activation and the start of tangential saline flow.

The mean diameter on detachment was almost equal for spontaneous detachment (no blow delivered to the bowl) and bubbles released as the result of a blow to the bowl (Fig. 3), with no significant difference between the two forms of detachment. However, when peak detachment occurred in the 0.5–1.0 mm bin for both spontaneous and blow-released bubbles, there was a trend, albeit non-significant, toward more blow-released bubbles in the larger diameter bin (17% more) and in the smaller diameter bin (14% more). This may imply that a blow delivered to the bowl had preference over spontaneous detachment for the release of large and small bubbles within the same range. The three smallest bubbles released on spontaneous detachment had diameters of 0.21, 0.32 and 0.34 mm, and on release by a blow delivered to the bowl this was 0.27, 0.31 and 0.34 mm. Delivering a blow to the bowl did not cause detachment of bubbles smaller than those which detached spontaneously, although there were many small bubbles available (empty bar, Fig. 3). The diameter of 16% of the observed stable bubbles was less than 0.21 mm, and none was released by a blow to the bowl. The diameter of the three largest stable bubbles, which were not released by a blow to the bowl, was 1.33, 1.27 and 0.96 mm.

3.2. Bubble detachment in the tangential flow protocol

In three sheep bubbles were produced in all four vessels, in two sheep in three vessels and in one sheep in two of the four vessels. The diameter of bubbles which became detached during the first 30 min, under calm conditions, was 0.81 ± 0.34 mm (mean ± SD), $n = 56$; during the second 30 min, under saline flow, this was 0.99 ± 0.36 mm, $n = 268$. Mean detachment diameter during flow was significantly greater than in the previous calm conditions ($P < 0.002$). Examples of bubble diameter on detachment for the four different blood vessels which produced bubbles both in the calm and flow conditions are shown in Fig. 4.

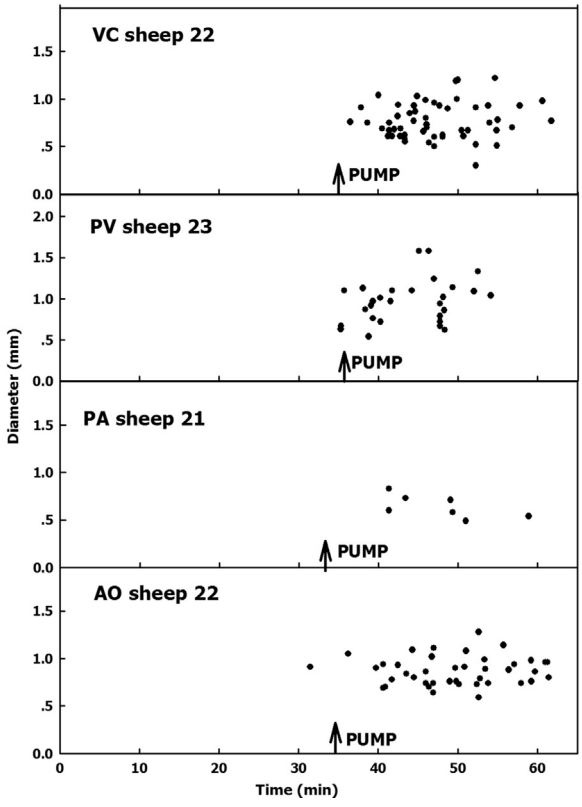

Fig. 5. Diameter of bubbles on detachment (tangential flow protocol) plotted as a function of time from decompression for four blood vessels with bubble production mainly during active saline flow. Other symbols are as in Fig. 4.

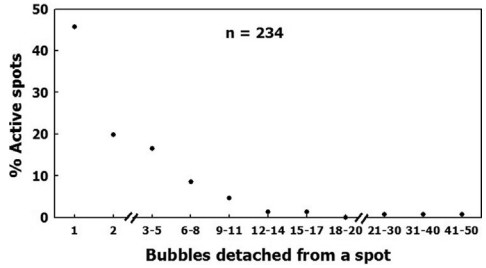

Fig. 6. Distribution of active spots according to their bubble detachments for all the 12 sheep throughout the entire 1 h. Total number of active spots is shown in the inset.

We checked for an immediate effect of flow, by recording bubbles that became detached within the first 3 s of flow activation. However, only one bubble detachment was recorded in that space of time. Thus no specific effect of flow could be demonstrated. In 40% of the vessels which produced bubbles, there were almost no bubble detachments during the first 30 min, under calm conditions, whereas large numbers of bubbles became detached during the second 30 min, under flow conditions. An example is given in Fig. 5. This phenomenon was not observed when conditions were calm in both periods.

3.3. Active spots

A large number of active spots produced only one bubble in the course of the 1-h observation, a smaller number produced two bubbles, and many fewer produced large numbers of bubbles. The distribution of active spots according to their bubble production is shown in Fig. 6, which summarises the data from all 12 sheep. The time which elapsed between the first and last detachment in two-bubble spots was 15.5 ± 11.7 min, $n = 29$, and in three-bubble spots 12.4 ± 13.5 min, $n = 7$.

3.4. Lipid staining

Lipid stains on the blood vessels were matched with the active spots. In many vessels, a match could be found between the red patch (stained for lipids) and the active spot. Five examples are given in Fig. 7, where an area containing the active spot (defined by bubble production), matches the lipid stain. A lipid-stained active spot could have the form of a circular dot, a blotch, or an elongated strip. Of 38 clearly stained active spots, only 21% of the matches were for spots producing 1–2 bubbles and 26% for spots producing 3–5 bubbles, whereas 53% of the matches were for spots which produced 6 bubbles or more. Thus the frequency of matched, stained active spots was inversely related to the percentage of spots producing 1–2, 3–5, or more bubbles: 66%, 17% and 17%, respectively (Fig. 6).

3.5. Distribution of bubble production

To evaluate the magnitude of bubble formation in the four blood vessels, we combined the data from the present study (bowl-striking and tangential protocols) with our previous study in calm conditions (Arieli and Marmur, 2014). Because there was almost no effect of striking the bowl, the data from the blow protocol and our previous report were combined as calm conditions ($n = 13$). Under calm conditions ($n = 13$) 2.2 ± 0.9 of the four vessels were defined as bubbling, whereas in the tangential flow protocol ($n = 6$) 3.5 ± 0.8 of the four were defined as bubbling. There were significantly more bubbling vessels in the flow protocol than in calm protocol ($P < 0.005$).

To assess the range and magnitude of bubble detachments in the four blood vessels, all detachments during the second sampling period (including those in non-bubbling vessels) were combined, and are presented in Fig. 8 in ascending order of bubble detachments per 1 cm^2. The second sampling period was chosen because we have shown (Arieli and Marmur, 2014) that following the

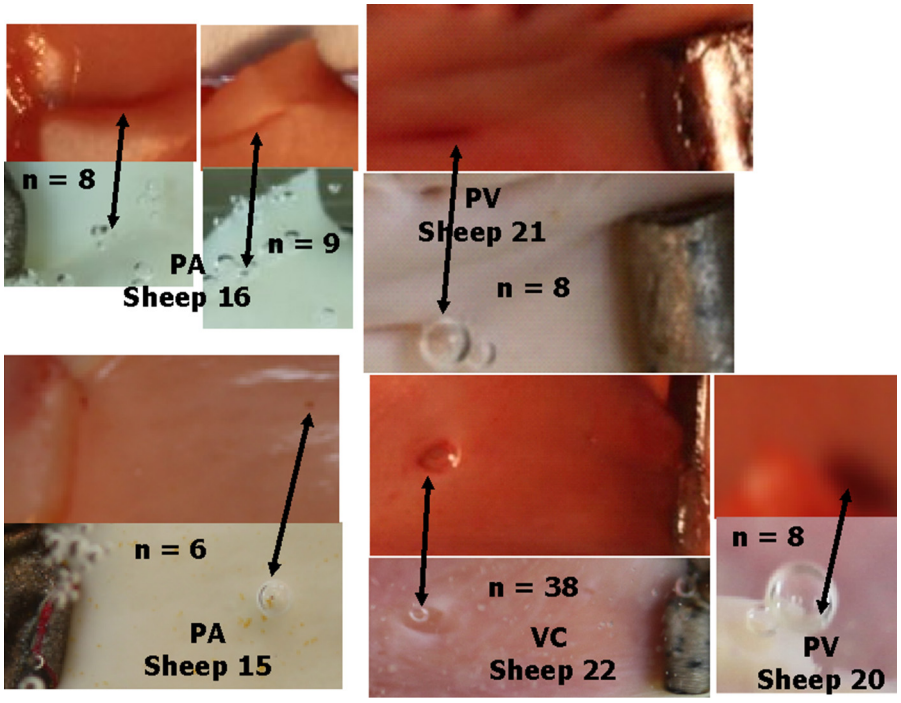

Fig. 7. Representative photographs of active spots from five sheep compared with staining for lipids in the same vessel. The lower photograph of each pair was taken while bubbles grew under saline at the active spot. The upper photograph is of the stained vessel. Arrows point to the matched sites. Sheep number and blood vessel are shown for each pair of photographs, together with the number of detached bubbles.

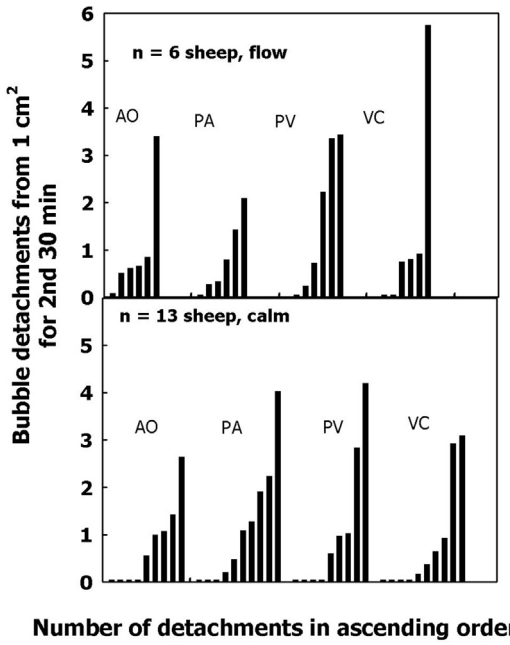

Fig. 8. Bubble detachments per 1 cm^2 from each blood vessel during the second 30 min, in ascending order of bubble production. Data from calm conditions (lower panel) and the flow protocol (upper panel) are shown.

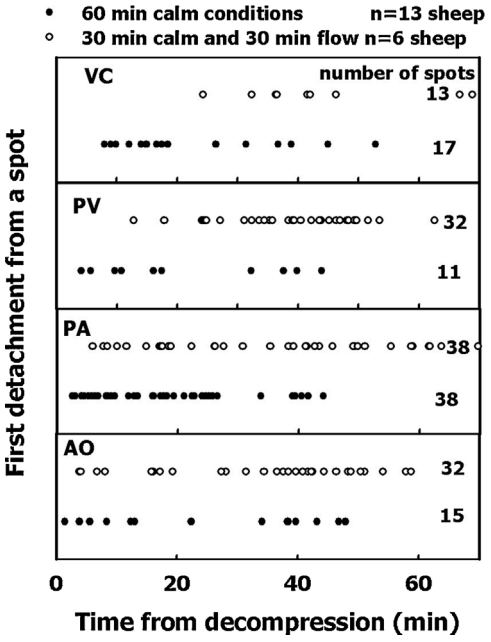

Fig. 9. Time from decompression until the first detachment from an active spot for 19 sheep plotted for the four blood vessels (symbols as in Fig. 2).

activation period, the time interval between bubble detachments became short and stabilised, and that it also took a considerable time for the first detachment after decompression. Data from both the tangential flow protocol and calm conditions are presented. Because tangential flow may enhance detachment, as well as bringing gas-rich saline to the vicinity of the blood vessel, the data were separated. The distributions for bubble detachment from the four blood vessels under calm or flow conditions seem similar to one another and between the blood vessels. There was no bubble production in 15 (39%) of 38 blood vessels in calm conditions, and in 4 (17%) of 24 in flow conditions. Detachments in the bubble-producing vessels ranged from 0.17 to 5.75 per 1 cm^2 during the second 30 min.

We showed (Arieli and Marmur, 2014) that it takes a mean of 12 min for a bubble to expand from some tens of microns to a diameter of 1 mm, concluding that it takes much longer for nanobubbles to become gas micronuclei. To assess the time taken for initiation of a spot (as we surmise, transformation of nanobubbles into gas micronuclei), we plotted the time to the first detachment from a defined active spot in Fig. 9. Thus spot initiation came about 12 min earlier than the detachment. Data for both calm and flow protocols are shown. It may be seen that the first bubble detachment from defined spots ranged over the whole hour, with fewer new active spots between 50 and 60 min post decompression in the calm protocol, but not in the flow protocol. When the number of active spots (shown to the left of each data symbol) is normalised for the number of sheep, the number of active spots in the flow protocol is much higher than in the calm protocol: 460%, 220%, 630% and 170% for AO, PA, PV and VC, respectively. The number of active spots per 1 cm^2 found in the flow protocol was significantly higher than in the calm protocol ($P < 0.006$). Total numbers of detached bubbles for a sheep (1 h, 4 vessels) were highly variable. For the 13 calm protocols in ascending order, the number of detached bubbles was 8, 13, 17, 21, 25, 27, 29, 39, 43, 69, 96, 124 and 153; for the flow protocol this was 7, 39, 44, 63, 71 and 98. There was no significant difference between the total number of detached bubbles per 1 cm^2 for the 2 protocols ($P = 0.056$).

4. Discussion

The match between Oil Red O-stained lipids and the active spots which produced bubbles confirmed our suggestion that bubbles nucleate and grow at hydrophobic spots on the luminal aspect of ovine large blood vessels. Because hydrophobicity was also demonstrated in other ovine blood vessels (Hills, 1992), the location of active hydrophobic spots on the luminal aspect of a broad range of blood vessels is probably a widespread phenomenon.

Delivering a blow to the bowl containing the blood vessel resulted in more detachments of small and large bubbles than on spontaneous detachment, but within the same size range, where the mean size on release did not differ between these groups. After striking the bowl, bubbles detached in the 1.5–2.0 mm bin (Fig. 3), in which one will not find any stable bubbles. This means that striking the bowl caused the release of all bubbles having a diameter greater than 1.5 mm. The percentage of bubbles released after striking the bowl is also higher in the 1.0–1.5 mm bin compared with the stable bubbles. However, the blow did not release bubbles as large as 1.33 and 1.27 mm, nor did it release bubbles smaller than those which detached spontaneously. The adhesion force at the active spots does not allow the blow to release tiny bubbles, and so striking the bowl may have the same effect on these bubbles as pulsatile blood flow, leaving them to continue to expand until they reach a sizeable volume.

In our previous study with silicon wafers, we demonstrated that the diameter of a bubble on tangential detachment was 80% of that on normal detachment. The tangential force on detachment was 50% compared with normal detachment (Arieli and Marmur, 2013a). However, bubble size on detachment in tangential flow (a diameter of 0.99 mm) was even greater than in calm conditions (0.81 mm). Therefore, the adhesion force for bubbles at the hydrophobic spot does not allow pulsatile blood flow with a mean linear velocity of 234 cm/min to detach bubbles having a diameter smaller than those which became detached in calm conditions. Using the Stokes equation, $Fd = 3\pi d\eta u$, where Fd is the drag force, d is the diameter, η is the dynamic viscosity, and u is the free stream velocity, the calculated maximal tangential force, assuming sinusoidal flow and a diameter of 1 mm, was calculated to amount

to 0.72×10^{-5} N. This value is less than half the normal force on detachment. Bubbles which were larger on detachment during flow compared with calm conditions may have grown faster due to the enriched gas in the flow of saline. It was noted that in the process of expanding to a diameter of 2 mm, a bubble was rocked back and forth by the pulsatile flow, but continued to adhere to the active spot. The size of a detached bubble, even under a powerful flow regime, may pose a considerable risk to the central nervous system.

The adhesion force for small bubbles (2–3 nl, diameter ~ 0.17 mm) within the mesenteric artery was about 10^{-7} N (Suzuki and Eckmann, 2003), which is two orders of magnitude smaller than the adhesion force of 4.5×10^{-5} N for the active spot in the present study and our previous investigation (Arieli and Marmur, 2014). This difference is probably related to the attachment force between a bubble and the hydrophilic endothelium in mesenteric arteries, compared with the attachment force between a bubble and a hydrophobic active spot in the present study.

Only in the flow protocol did no bubble detachments occur in calm conditions, although bubbles did appear under flow conditions (in 40% of vessels, Fig. 5). Thus the number of bubbling vessels increased from 2.2 to 3.5 of 4 between the calm and flow protocols. The mean number of active spots increased almost fourfold between the calm and flow protocols (Fig. 9, normalising for sheep number × 13/6). We suggest that the increased concentration of dissolved gas near the vessel during flow (mixing of the high gas concentration in the upper saline with the low gas concentration in the lower saline, Appendix 1) enhanced the initiation of active spots and the subsequent transformation, as we surmised, of nanobubbles into gas micronuclei. We have previously shown that the density of bubbles on a hydrophobic silicon wafer after decompression increased with elevation of the preceding exposure pressure and gas load (Arieli and Marmur, 2013a). The relation between gas load and increased bubble score is well known in diving. We might suggest that after decompression, when the gas load near the blood vessel was elevated, it initiated more active spots, with a resultant increase in bubble formation.

The initiation of active spots was observed throughout the entire 1-h observation period (Fig. 9). Thus the initiation of the active spot is the slow process, compared with bubble growth, which takes about 12 min (Arieli and Marmur, 2014) and is the fast process.

A considerable number of active spots produced only a few bubbles (Fig. 6). The time between the first and last detachment for these spots was much shorter (15.5 min for 2-bubble spots and 12.4 min for 3-bubble spots) than the 1-h period during which measurements were made. Despite the high prevalence of spots which produced 1–2 bubbles (66%, Fig. 6), observable staining for these spots was low, 21% of all the stained spots. Active spots from which more than six bubbles detached constituted 53% of the stained spots, but only 17% of the total active spots. One explanation for this may be that the area of active spots producing small numbers of bubbles is too small to be seen in the enlarged photograph. It is also possible that the phospholipids from these active spots may have been carried away along with the detached bubbles. A similar finding was presented by Hills and Butler (1981), when the pulmonary vasculature of the dog was flushed with microbubbles containing serum. The outflow contained surfactant which was carried away by the bubbles. We suggest that the surfactant composing the active spot may cling to the bubble, and be carried away together with the bubble on detachment. In this way, the surfactant in the smaller and less productive active spots would be depleted, and the spot would no longer be active. This process may provide an explanation for acclimation to diving. Experienced divers will produce fewer bubbles than the novice, and will thus be less prone to decompression sickness (Sayer et al., 2008; Pontier et al., 2009; Zanchi et al., 2014). Presumably bubbles produced during their long diving history have eliminated some of their active spots.

The formation of bubbles in the arterial circulation after decompression necessitates a reappraisal of our view that decompression sickness is a venous disease. The present finding that bubbles continue to grow even under a flow regime and are not swept away when they are small stresses the possible role of significant numbers of large arterial bubbles in neurologic decompression sickness. It also supports our previous suggestion (Arieli and Marmur, 2014) that symptoms of neurologic decompression sickness can occur without arterialisation of venous blood, either via a patent foramen ovale (PFO) or intrapulmonary arteriovenous anastomoses (IPAVA) (Madden et al., 2015). Therefore the common use of the term "air embolism" with reference to the arterialisation of bubbles does not cover all arterial bubbles. Major decompression illness (DCI) has been shown to be related to the magnitude of patency of a patent foramen ovale (PFO) (Torti et al., 2004). However, 36% of divers who suffered DCI had no PFO. Severe cases of neurologic decompression sickness may occur immediately on surfacing from a dive or within a few minutes (Elliott and Moon, 1993). Neurologic decompression sickness has been divided into two categories: Type A, the more severe form and Type B, the milder form Grover et al. (2007). Although a correlation has been shown between Type A and PFO, none was found for Type B (Koch et al., 2008). Germonpré et al. (1998) found an association between cerebral DCS and PFO, at the same time, however, claiming there were exceptionally high numbers of unexplained DCS episodes. In their analysis of DCS in divers, Wilmshurst et al. (1989) found that 66% of the divers in whom neurologic DCS appeared within half an hour of the dive had a PFO. Of the divers in whom neurologic DCS appeared between half an hour and 48 h after the dive, only 24% had a PFO. High percentages of neurologic DCS cannot necessarily be related to a PFO.

The source we have suggested for bubble production after decompression, active spots on the luminal aspect of blood vessels, correlates well with what we see among divers: 1. Acclimation, as described above, when phospholipids were swept away by bubbles; 2. Variable sensitivity to decompression stress (bubblers vs. non-bubblers). In 1 h, 53% of sheep produced 0–40 bubbles, 26% produced 40–80 bubbles, 10.5% produced 80–120 bubbles, and 10.5% produced 120–160 bubbles; 3. Increased bubble production with increasing gas load, i.e., initiation of active spots with increasing gas load; 4. Increased bubble production in the second dive on the same day matches activation of active spots after the first few bubbles became detached (Arieli and Marmur, 2014); 5. Unexplained neurologic DCI, and no evidence of a left-to-right shunt, which may be explained by bubble production in the arterial circulation.

5. Conclusion

On decompression, bubbles nucleate from nanobubbles permanently resident at active hydrophobic spots on the luminal aspect of diverse blood vessels. These bubbles grow to a mean size of 1 mm in diameter in the face of pulsatile blood flow, before their release into the bloodstream. The present suggested source of bubble formation correlates with various features of diving, and represents a direct risk of neurologic decompression sickness.

Acknowledgements

The authors thank Mr. R. Lincoln for skillful editing of the manuscript. This study was supported in part by a grant from the IDF Medical Corps and the Israel MOD (1105-2012).

Appendix A.

A.1. Gas concentration

Let us assume an initial distribution of the following kind:

$$f(x,0) = n_0, \quad 0 < x < L$$

$$n_1, \qquad L < x$$

Also, at $x=0$ we assume an infinite potential wall which molecules cannot pass. To overcome this problem, we need to find a system in which for $x>0$ the distribution is similar to $f(x,0)$, but in which for each molecule leaving our box from $x=0^+$ to $x=0^-$, another molecule arrives from $x=0^-$ and enters the box at $x=0^+$ to replace the molecule which has left.

Let us consider the next function:

$$g(x,0) = n_0, \quad -L < x < L$$

$$n_1, \qquad |x| > L$$

From considerations of symmetry, we can see that for every molecule that goes from $x=0^-$ to $x=0^+$ there will be a "mirror" molecule that goes from $x=0^-$ to $x=0^+$.

The solution for $g(x,t)$ is given by the convolution with $\frac{1}{\sqrt{4\pi Dt}}\exp\left(-x^2/4Dt\right)$.

$$g(x,t) = \int_{-\infty}^{\infty} g(x-y,0)\,\frac{\exp\left(-y^2/4Dt\right)}{\sqrt{4\pi Dt}}\,dy$$

We are interested only in $g(0,t)$. So, remembering that the function is symmetric in x and changing variables $\left\{u = x/\sqrt{4Dt},\, du = dx/\sqrt{4Dt}\right\}$ we obtain:

$$g(0,t) = \frac{2}{\sqrt{\pi}}\left[\int_0^{L/\sqrt{4Dt}} n_0\exp\left(-u^2\right)du + \int_{L/\sqrt{4Dt}}^{\infty} n_1\exp\left(-u^2\right)du\right]$$

For each $L/\sqrt{4Dt}$ the integral was calculated via Wolframalpha.

For example, for $L=2.5\,\text{cm}$, $t=72{,}000\,\text{s}$ and $D=2.01\times10^{-5}\left(\text{cm}^2/\text{s}\right)$ we get $L/\sqrt{4Dt}\approx 1.03907$. For $n_0=0.1\times n_1$ we obtain the solution:

$$g(0.72000\,\text{s}) =$$

$$= \frac{2n_1}{\sqrt{\pi}}\left[\int_0^{1.03907} 0.1\times\exp\left(-u^2\right)du + \int_{1.03907}^{\infty} 1\times\exp\left(-u^2\right)du\right]$$

$$\approx 0.2275\times n_1$$

Gas tension at the tissue surface after 20 h would amount to saturation at a depth of 12.75 msw (228 kPa).

References

Arieli, R., Marmur, A., 2011. Decompression sickness bubbles: are gas micronuclei formed on a flat hydrophobic surface? Respir. Physiol. Neurobiol. 177, 19–23.

Arieli, R., Marmur, A., 2013a. Dynamics of gas micronuclei formed on a flat hydrophobic surface, the predecessors of decompression bubbles. Respir. Physiol. Neurobiol. 185, 647–652.

Arieli, R., Marmur, A., 2013b. Evolution of bubbles from gas micronuclei formed on the luminal aspect of ovine large blood vessels. Respir. Physiol. Neurobiol. 188, 49–55.

Arieli, R., Marmur, A., 2014. Ex vivo bubble production from ovine large blood vessels: size on detachment and evidence of active spots. Respir. Physiol. Neurobiol. 200, 110–117.

Elliott, D.H., Moon, R.E., 1993. Manifestations of the decompression disorders. In: Bennett, P.B., Elliott, D.H. (Eds.), The Physiology and Medicine of Diving. , fourth ed. W.B. Saunders Company Ltd, London, UK, pp. 484–488.

Germonpré, P., Dendale, P., Unger, P., Balestra, C., 1998. Patent foramen ovale and decompression sickness in sports divers. J. Appl. Physiol. 84, 1622–1626.

Grover, I., Reed, W., Neuman, T., 2007. The SANDHOG criteria and its validation for the diagnosis of DCS arising from bounce diving. Undersea Hyperb. Med. 34, 199–210.

Hills, B.A., 1992. A hydrophobic oligolamellar lining to the vascular lumen in some organs. Undersea Biomed. Res. 19, 107–120.

Hills, B.A., Butler, B.D., 1981. Migration of lung surfactant to pulmonary air emboli. In: Bachrach, A.J., Matzen, M.M. (Eds.), Underwater Physiology VII. Proceedings of the Seventh Symposium on Underwater Physiology. Undersea Medical Society, Bethesda, MD, pp. 741–751.

Koch, A.E., Kirsch, H., Reuter, M., Warninghoff, V., Rieckert, H., Deuschl, G., 2008. Prevalence of patent foramen ovale (PFO) and MRI-lesions in mild neurological decompression sickness (Type B-DCS/AGE). Undersea Hyperb. Med. 35, 197–205.

Madden, D., Ljubkovic, M., Dujic, Z., 2015. Intrapulmonary shunt and SCUBA diving: another risk factor? Echocardiography 32 (Suppl 3), S205–S210.

Pontier, J-M., Guerrero, F., Castagna, O., 2009. Bubble formation and endothelial function before and after 3 months of dive training. Aviat. Space Environ. Med. 80, 15–19.

Sayer, M.D.J., Akroyd, J., Williams, G.D., 2008. Comparative incidences of decompression illness in repetitive, staged, mixed-gas decompression diving: is 'dive fitness' an influencing factor? Diving Hyperb. Med. 38, 62–67.

Snyder, G.K., 1973. Erythrocyte evolution: the significance of the Fåhraeus-Lindqvist phenomenon. Respir. Physiol. 19, 271–278.

Suzuki, A., Eckmann, D.M., 2003. Embolism bubble adhesion force in excised perfused microvessels. Anesthesiology 99, 400–408.

Torti, S.R., Billinger, M., Schwerzmann, M., Vogel, R., Zbinden, R., Windecker, S., Seiler, C., 2004. Risk of decompression illness among 230 divers in relation to the presence and size of patent foramen ovale. Eur. Heart J. 25, 1014–1020.

Tyrrell, J.W.G., Attard, P., 2001. Images of nanobubbles on hydrophobic surfaces and their interactions. Phys. Rev. Lett. 87, 176104-1–176104-4.

Wilmshurst, P.T., Byrne, J.C., Webb-Peploe, M.M., 1989. Relation between interatrial shunts and decompression sickness in divers. Lancet 2, 1302–1306.

Yang, S., Dammer, S.M., Bremond, N., Zandvliet, H.J.W., Kooij, E.S., Lohse, D., 2007. Characterization of nanobubbles on hydrophobic surfaces in water. Langmuir 23, 7072–7077.

Zanchi, J., Ljubkovic, M., Denoble, P.J., Dujic, Z., Ranapurwala, S., Pollock, N.W., 2014. Influence of repeated daily diving on decompression stress. Int. J. Sports Med. 35, 465–468.